ACS Catalysis

pubs.acs.org/acscatalysis

Letter

Crystallographic Characterization of the Carbonylated A-Cluster in Carbon Monoxide Dehydrogenase/Acetyl-CoA Synthase

Steven E. Cohen, Mehmet Can, Elizabeth C. Wittenborn, Rachel A. Hendrickson, Stephen W. Ragsdale, and Catherine L. Drennan*

Cite This: *ACS Catal.* 2020, 10, 9741−9746

Read Online

ACCESS | Metrics & More | Article Recommendations | Supporting Information

ABSTRACT: The Wood−Ljungdahl pathway allows for autotrophic bacterial growth on carbon dioxide, with the last step in acetyl-CoA synthesis catalyzed by the bifunctional enzyme carbon monoxide dehydrogenase/acetyl-CoA synthase (CODH/ACS). ACS uses a complex Ni−Fe−S metallocluster termed the A-cluster to assemble acetyl-CoA from carbon monoxide, a methyl moiety and coenzyme A. Here, we report the crystal structure of CODH/ACS from *Moorella thermoacetica* with substrate carbon monoxide bound at the A-cluster, a state previously uncharacterized by crystallography. Direct structural characterization of this state highlights the role of second sphere residues and conformational dynamics in acetyl-CoA assembly, the biological equivalent of the Monsanto process.

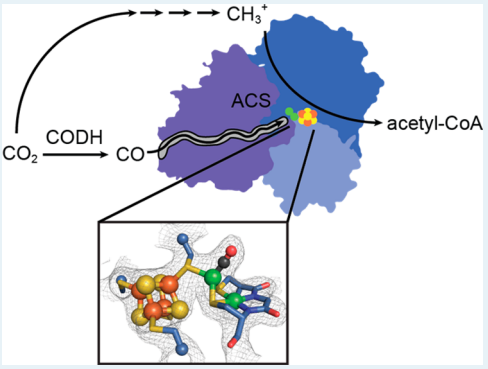

KEYWORDS: *CODH, ACS, Wood−Ljungdahl, acetogenesis, metalloenzymes, carbon monoxide, acetyl coenzyme A, X-ray crystallography*

Carbon monoxide (CO) dehydrogenase/acetyl-CoA synthase (CODH/ACS) is a bifunctional enzyme in the Wood−Ljungdahl pathway that allows for the autotrophic growth of acetogenic bacteria on carbon dioxide (CO_2) and a reducing source.[1] *Moorella thermoacetica* CODH/ACS is a 310 kDa protein with a dimeric CODH core and ACS subunits on either end (Figure 1). The $NiFe_4S_4$ C-cluster of the CODH component catalyzes the reversible two-electron reduction of CO_2 to CO, using Fe_4S_4 B- and D-clusters for electron transfer.[2] CO travels through an internal gas tunnel that connects the active site of each CODH subunit to that of an ACS subunit.[3,4] ACS then catalyzes the reversible condensation of CO, provided by CODH, with a methyl group donated by a corrinoid iron−sulfur protein (CFeSP), and coenzyme-A (CoA), to form acetyl-CoA (Scheme 1).[5−7] This reaction is the biological equivalent of the Monsanto process. Although a consensus mechanism is emerging for CODH,[8−10] the mechanistic details of ACS remain elusive and contentious.

ACS catalyzes acetyl-CoA synthesis using a complex metallocofactor called the A-cluster (Scheme 1).[11−13] This cluster consists of a Fe_4S_4 cubane connected to a dimetal center through a cysteine thiol.[3] The dimetal center contains Ni−Ni in the active state,[14−16] with the nickel proximal to the Fe_4S_4 cluster, Ni_p, able to adopt different geometries[17,18] and the distal Ni, Ni_d, fixed in a square planar arrangement through its coordination to the protein backbone and cysteine side chains (Scheme 1).[3] Both carbonylation and methylation are proposed to occur at one Ni site, Ni_p.[9,12,17,19,20] The carbonylated state of the A-cluster is associated with an electron paramagnetic resonance (EPR) signal, the A_{NiFeC} species,[12] which is thought to consist of Ni_p^{+}−CO bound to Ni_d^{2+} and the $[Fe_4S_4]^{2+}$ cluster. The carbonylated A-cluster has been probed by electron nuclear double resonance,[21] Mössbauer,[13] infrared,[22] and extended X-ray absorption fine structure (EXAFS)[19] spectroscopies, but this state has never been crystallographically observed.

A different conformation of the three-domain ACS subunit appears necessary for carbonylation rather than for methylation.[3,4,17] A-cluster carbonylation requires that CO can travel through the gas tunnel that runs within domain 1 of ACS to reach domain 3 where the A-cluster is bound.[4] This closed ACS conformational state has been captured crystallographically in *M. thermoacetica* CODH/ACS,[3,17] showing ACS domains 1 and 3 packed against each other with the A-cluster at the end of a gas tunnel that was mapped through use of xenon-derivatized crystals (Figure 1A).[4] In contrast, A-cluster methylation requires an open state of ACS in which domain 3 is swung away from domain 1, allowing CFeSP to bind and deliver the methyl group. Partially open states of the bifunctional *M. thermoacetica* CODH/ACS (Figure 1B) and

Received: July 10, 2020
Revised: August 10, 2020
Published: August 10, 2020

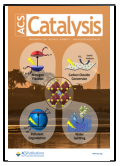

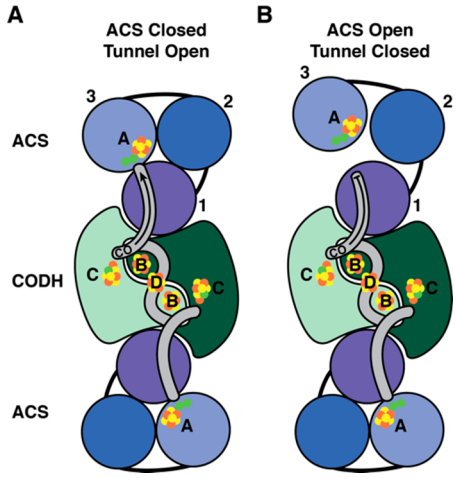

Figure 1. Cartoon structures of CODH/ACS. (A) CODH/ACS with both ACS subunits in the closed conformation and both CO tunnels open. (B) CODH/ACS with the top ACS subunit in a partially open conformation and the accompanying CO tunnel closed. The CODH dimer is colored in light and dark green, and ACS domains 1, 2, and 3 are colored in violet, navy, and light blue, respectively. Metalloclusters are shown as spheres with iron, sulfur, and nickel in orange, yellow, and green, respectively.

Scheme 1. A-Cluster Reaction and Structure

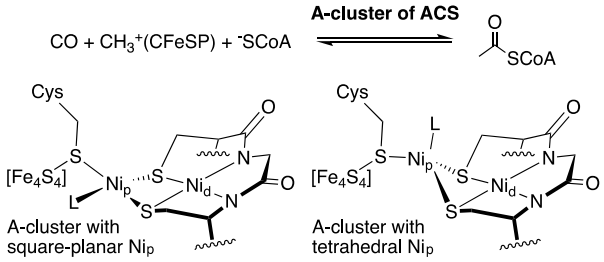

monofunctional *Carboxydothermus hydrogenoformans* ACS have been captured by crystallography, but they are not sufficiently open for CFeSP binding.[17,18] A fully open ACS state has not yet been visualized.

To further investigate the structure of the A-cluster with CO bound, we have solved the 2.47 Å resolution crystal structure of CO-treated CODH/ACS from *M. thermoacetica*, the prototypic CODH/ACS enzyme. We compare this crystal structure, which was derived using CODH/ACS that was purified from the native *M. thermoacetica* organism, with previously published DFT- and EXAFS-derived models of the A-cluster in the A_{NiFeC} state,[19] which utilized a heterologously expressed ACS subunit. Additionally, these structural data reveal the conformations of second sphere residues when the A-cluster is carbonylated. Using these data, an extended model for the role of conformational rearrangements in catalysis is presented.

GENERATION OF THE A_{NiFeC} SPECIES IN SOLUTION UNDER CRYSTALLIZATION CONDITIONS

EPR spectroscopy was used to investigate whether the characteristic A_{NiFeC} EPR signal of the carbonylated form of the A-cluster is generated in solution in the presence of the components of the crystallization buffer (Figure 2A).[12] As-isolated CODH/ACS shows a weak EPR signal corresponding

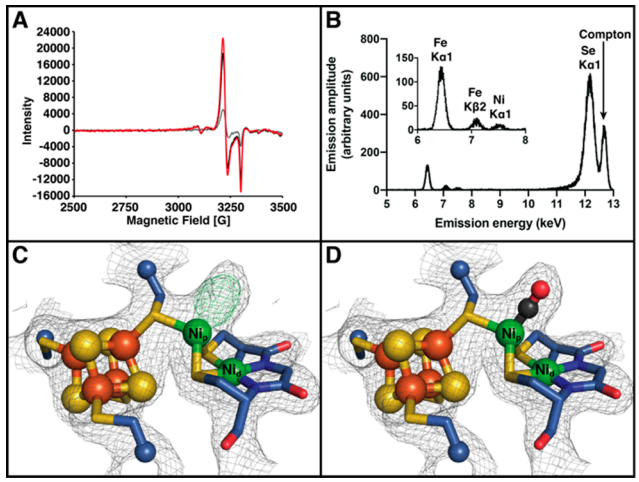

Figure 2. Spectroscopic and crystallographic characterization of the carbonylated A-cluster. (A) EPR spectra of CODH/ACS in storage buffer (gray), 60:40% (v/v) storage buffer:crystallization solution (black), and CO-sparged 60:40% (v/v) storage buffer:crystallization solution (red). *g*-Values are 2.08, 2.07, and 2.03, respectively. (B) Energy dispersion X-ray spectroscopy of crystals showing no metal contamination. (C) The A-cluster refined without CO. (D) The A-cluster refined with CO (red/gray). Atom colors as in Figure 1. $2F_O - F_C$ simulated annealing composite omit maps contoured at 1σ and shown as gray mesh. $F_O - F_C$ maps contoured at $\pm 4.0\sigma$ and shown as green and red mesh, respectively.

to 0.12 spins per ACS monomer, indicating the presence of trace CO in the protein stock. The addition of precipitant solution causes a substantial increase in the A_{NiFeC} signal, corresponding to 0.37 spins per ACS monomer, consistent with the presence of CO as an impurity in the crystallization reagent polyethylene glycol. Sparging the EPR sample with CO prior to addition of CODH/ACS further increases the signal to 0.44 spins per ACS monomer. Issues with protein precipitation led to incomplete carbonylation, however, these spectroscopic data support our ability to crystallographically capture the carbonylated state of the A-cluster that gives rise to the A_{NiFeC} state.

CARBON MONOXIDE IS BOUND AT THE A-CLUSTER OF ACS

CODH/ACS crystals were grown in an anaerobic chamber as described previously,[3,4,23] and using the same crystallization conditions tested above for compatibility with A-cluster carbonylation. To obtain the A_{NiFeC} state, crystals were treated with sodium dithionite and CO prior to cryo-cooling and data collection. Because the proximal metal site in the A-cluster is highly susceptible to metal exchange by Cu and Zn ions during growth and/or protein purification of CODH/ACS from its native *M. thermoacetica*,[3,17] energy dispersion X-ray spectroscopy (EDS) was used to confirm that the CODH/ACS crystals used in this study contained Ni−Fe−S exclusively. No transition metal contamination was detected (Figures 2B and S1), making this the first crystal structure of the prototypic CODH/ACS from *M. thermoacetica* to exclusively contain dinickel A-clusters. As has been observed previously, the 310 kDa CODH/ACS tetrameric complex crystallized in space group *P*1 with two tetrameric molecules in the asymmetric unit (Figure S2A). The ACS subunits of one tetramer participate in stronger lattice contacts, stabilizing the closed conformation. The ACS subunits of the other tetramer are more poorly

https://dx.doi.org/10.1021/acscatal.0c03033
ACS Catal. 2020, 10, 9741−9746

resolved, and likely sample a conformational range, based on the higher *B*-factors in these chains (Figure S2B). Data collection, processing, and refinement statistics are summarized in Table S1.

The metals of the A-cluster are arranged as expected (Figure 2C). In contrast to the only other structure of CODH/ACS that contains dinickel,[17] the density around Ni_p in our structure does not indicate a mixture of square planar and tetrahedral geometries for Ni_p. Instead, electron density maps are consistent with a ligand-bound Ni_p that is exclusively tetrahedral (Figure S3A). In particular, when Ni_p is refined with square planar geometry as observed with partial occupancy in the previous CODH/ACS structure and with full occupancy in the structure of monofunctional ACS from *C. hydrogenoformans*,[17,18] negative difference density at Ni_p appears, indicating that Ni_p should be repositioned (Figure S3B). In contrast, no negative difference density is present when Ni_p is refined with tetrahedral geometry (Figure S3A). In all cases, a positive $F_O - F_C$ electron density peak is present by Ni_p, indicating the presence of a single bound ligand (Figures 2C and S3). The size and shape of the peak are consistent with a diatomic molecule bound in a linear mode to a tetrahedral Ni_p. Refinement of a CO molecule at this site results in no positive or negative peaks in the $F_O - F_C$ electron difference density maps when contoured at $\pm 4\sigma$ (Figure 2D), indicating that the observed density is consistent with one CO molecule as the ligand to a tetrahedral Ni_p.

The A-cluster was refined as carbonylated at Ni_p for three of the four ACS chains. The carbonylated A-clusters were parametrized for crystallographic refinement according to published DFT- and EXAFS-derived models of A_{NiFeC} that were based on the heterologously expressed ACS subunit.[19] Refinement using these parameters generates structures that show good agreement with the X-ray diffraction maps. Relaxing A-cluster restraints during refinement results in deviations from published distances by no more than 0.1−0.2 Å, which is within error of the resolution of the crystallographic data. All three A-clusters display similar geometries, bond distances (within 0.15 Å), and bond angles (within 3.7°) (Tables S2 and S3). CO bound to Ni_p with tetrahedral geometry has a C−Ni_p distance of 1.63 Å, shorter than the DFT- and EXAFS-derived values of 1.75 and 1.77 Å,[19] but within the error associated with a 2.47-Å resolution crystal structure.

THE STRUCTURE OF CODH/ACS WITH CO BOUND IS A CLOSED ACS CONFORMATION

The ACS subunits in our structure of CO-treated CODH/ACS are in the closed conformation with domain 1 (residues 2−311) packed against domain 3 (residues 501−729), protecting the carbonylated A-cluster from solvent (Figure S4). As previously noted,[3,17,20,23] this closed ACS conformation influences the positioning of three important A-cluster second-sphere residues: Phe229 and Ile146 from domain 1 and Phe512 from domain 3. Here we find that Phe512 is positioned away from Ni_p, which leads to the CO gas tunnel being open, and creates room for the CO traveling through the gas tunnel to bind Ni_p with tetrahedral geometry (Figure 3A). Phe229 appears to stabilize this tetrahedral geometry by stacking against the CO, whereas Ile146 packs against the A-cluster, hindering Ni_p from adopting the square-planar geometry that has been proposed to be necessary for methylation (Figure 3C).[17] This position of Ile146 also blocks

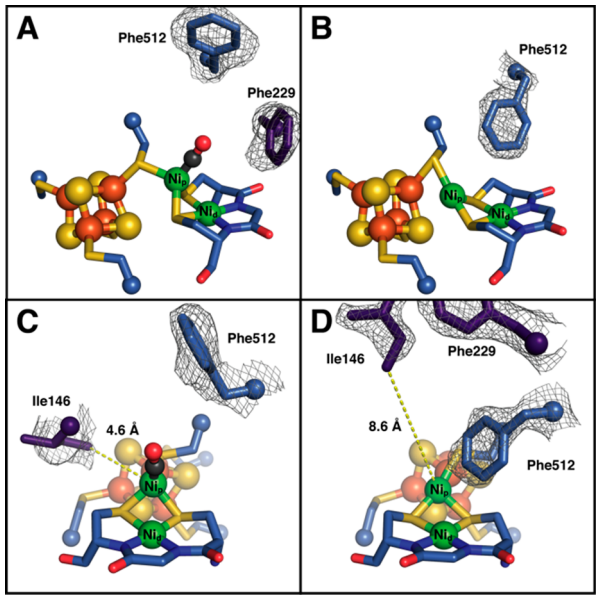

Figure 3. Open and closed conformations of ACS affect residue positions and A-cluster geometry. (A) In the closed ACS conformation observed here and previously, Phe512 is positioned away from the A-cluster and the proximal metal shows tetrahedral coordination. (B) In an open ACS conformation (PDB 1OAO), Phe512 swings toward the A-cluster and Ni_p adopts square planar coordination as one of two coordination geometries observed. An unidentified ligand observed in 1OAO has been modeled as water, consistent with partial solvent exposure of the A-cluster. (C) Alternative view of panel A showing Ile146 in close proximity to Ni_p. (D) Alternate view of panel B, showing that Ile146 is positioned away from the A-cluster in the open conformation. $2F_O - F_C$ simulated annealing composite omit maps contoured at 1σ. Atoms colored as in Figure 1.

binding of a second ligand to Ni_p. By comparison, in the previously determined partially open ACS structure,[17] the CO gas tunnel is closed and Phe512 is swung toward the A-cluster, sterically occluding a fourth ligand from binding in a tetrahedral geometry (Figure 3B). Phe512 is able to adopt this swung-in position due to the displacement of Phe229 away from the A-cluster. Ile146 is also now far (~8 Å) from Ni_p where it can no longer prevent binding of a second ligand and/or the adoption of square planar geometry (Figure 3D).[17,18] The A-cluster geometry observed in this work supports the previously proposed model that the closed conformation is the carbonylation-ready state of CODH/ACS.[9,17]

In summary, the A-cluster of CODH/ACS performs the impressive task of assembling acetyl-CoA from a molecule of CO, a methyl group, and a molecule of CoA. Here the first crystal structure of a CO-bound state of the A-cluster shows Phe229 stacked against the CO and Phe512 is swung away from the A-cluster, allowing Ni_p to adopt tetrahedral geometry with the fourth coordination site occupied by the CO ligand. No evidence for a square planar Ni_p conformation is observed, potentially due to the close positioning of Ile146. Thus, our structure is consistent with the proposal that residues Phe512, Phe229, and Ile146 of ACS act as steric gatekeepers to the A-cluster, favoring coordination geometries associated with either carbonylation or methylation (Scheme 2).[20,24] Notably, Phe512 and Phe229 are highly conserved, but can also be tyrosine, and Ile146 is always an amino acid with a branched side chain (Ile 48%, Val 46%, Thr 4%, Leu 2%).

https://dx.doi.org/10.1021/acscatal.0c03033
ACS Catal. 2020, 10, 9741−9746

Scheme 2. Structural Model for ACS Activity[a]

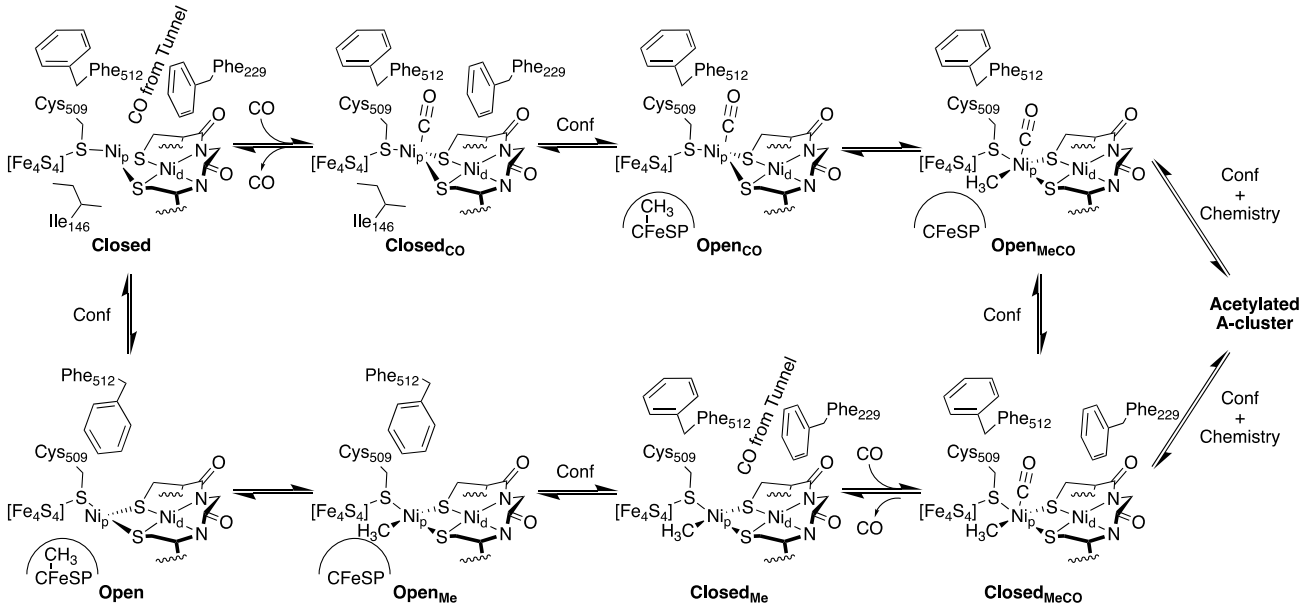

[a]"Conf" indicates conformational change. Closed and open states previously reported as PDB 1MJG and PDB 1OAO, respectively. $Closed_{CO}$ state reported in this paper. $Open_{CO}$, $Open_{MeCO}$, $Open_{Me}$, $Closed_{Me}$, and $Closed_{MeCO}$ are hypothetical states described in text.

This finding highlights a paradox in the current structure-based model for ACS activity. Pulse-chase studies indicate that ACS can proceed through a random sequential mechanism, with either CO or a methyl group binding the A-cluster first.[25] Therefore, there must be a mechanism for the carbonylated A-cluster to be methylated and for the methylated A-cluster to be carbonylated. However, the current model is that the open ACS conformation is methylation-competent but occludes carbonylation, and the closed ACS conformation is carbonylation-competent, but occludes methylation. This model is incompatible with the fact that a methyl group and CO must both bind the A-cluster.

To address this inconsistency, there must be additional uncharacterized structural states of ACS in its catalytic cycle (Scheme 2). ACS adopts the open and closed conformations through motions of the domains of ACS (Figure 1).[3,17] These structural rearrangements are coupled to motion in Phe512, Phe229, and Ile146, and the A-cluster, allowing for carbonylation of the Closed conformation to generate the $Closed_{CO}$ state characterized in this paper and methylation of the Open conformation to generate the $Open_{Me}$ state. For either of these states to then bind their next substrate, there must be rearrangements to adopt conformations not previously observed in ACS. The $Closed_{CO}$ state must open in a way that allows for CFeSP binding and subsequent methylation. However, this state cannot be the crystallographically observed Open conformation because Phe512 would clash with CO. Therefore, there must be an uncharacterized $Open_{CO}$ state distinct from the Open state that allows for methylation of the previously carbonylated A-cluster to generate an $Open_{MeCO}$ state. Likewise, the $Open_{Me}$ state must be able to close to form a $Closed_{Me}$ state such that Ile146 does not clash with the methyl group and the gas tunnel from CODH is intact to allow for CO to bind and generate the $Closed_{MeCO}$ state. Both the $Closed_{MeCO}$ and $Open_{MeCO}$ states might undergo further conformational rearrangements to condense the methyl and carbonyl groups into an acetyl moiety and/or to bind CoA for thiolation of the acetyl group to form acetyl-CoA.

There is not general agreement that ACS proceeds through a random sequential mechanism. Thus, it is important to note that the bottom pathway in Scheme 2 can be used to describe the structural states in the alternative proposal, favored by Gencic et al.,[20] in which methylation is the first step in an ordered sequential mechanism.

The structure presented here also provides insight into the observation that CO can be both a substrate and an inhibitor of the A-cluster depending on the CO concentration.[26] In this structure, we find CO bound to Ni_p at the end of the gas tunnel in an alcove created by Phe229, leaving open the coordination site where methylation is proposed to occur. CO cannot rearrange into this site in the Closed ACS state due to the positioning of Ile146. In this structural state, CO is not an inhibitor. However, when ACS opens, Ile146 would no longer block the putative methylation site, and the bound CO molecule could rearrange into this site and/or a second CO molecule from solution could bind. Although rearrangement of a bound CO can be reversed, the binding of a second CO would be expected to inhibit methylation. Given this apparent importance of conformational flexibility on the availability of A-cluster coordination sites, the exact conditions of an experiment could shift the equilibrium of ACS conformers thus altering the findings. In other words, although the A-cluster is an incredible biological catalyst, it would be a mistake to think of it only as a collection of inorganic elements, the protein dynamics are key to catalysis.

In addition to disagreements over random versus sequential mechanisms, there has been a long-standing debate over whether the A-cluster operates by a paramagnetic or a diamagnetic mechanism.[9,27−29] Briefly, the previously proposed diamagnetic mechanism invokes a resting, formally neutral Ni_p species, which can undergo carbonylation or methylation to form Ni_p−CO or Ni_p^{2+}−CH_3 species.[29] The paramagnetic mechanism proposes a resting Ni_p^{+} species,

https://dx.doi.org/10.1021/acscatal.0c03033
ACS Catal. 2020, 10, 9741−9746

which can form Ni_p^{+}−CO or Ni_p^{3+}−CH_3 species. The formation of the A_{NiFeC} state when as-isolated CODH/ACS is reduced and carbonylated has been taken as evidence of a paramagnetic mechanism.[12,30−32] Further support for a paramagnetic mechanism has come from a nickel-substituted azurin model that has been recently shown to adopt Ni^{+}, Ni^{2+}, and Ni^{3+} oxidation states, and to generate Ni^{+}−CO species and Ni^{3+}−CH_3 species.[33−35] This crystal structure shows the expected tetrahedral geometry for Ni^{+} with CO bound.[19] We do not observe any rearrangements of the A-cluster or of the protein that could be invoked to explain stabilization of Ni_p in a Ni^0 state, a state that currently has no precedent in a biological system.

In conclusion, although there are still a number of unanswered questions about the A-cluster mechanism, both spectroscopic[19] and crystallographic data are now available, depicting how CO, generated from CO_2 at the C-cluster, is captured by the A-cluster in CODH/ACS as part of the ultimate step of autotrophic acetyl-CoA synthesis through the Wood−Ljungdahl pathway. With increased interest in the biological fixation of CO_2, an understanding of the complex metallocatalyst responsible for assembling acetyl-CoA takes on new importance.

■ ASSOCIATED CONTENT

Supporting Information

The Supporting Information is available free of charge at https://pubs.acs.org/doi/10.1021/acscatal.0c03033.

Experimental procedures, spectroscopic data, crystallographic data collection and refinement statistics, and further structural analysis (PDF)

■ AUTHOR INFORMATION

Corresponding Author

Catherine L. Drennan − *Department of Chemistry and Department of Biology, Massachusetts Institute of Technology, Cambridge, Massachusetts 02139, United States; Howard Hughes Medical Institute, Cambridge, Massachusetts 02139, United States; Bio-inspired Solar Energy Program, Canadian Institute for Advanced Research, Toronto, ON M5G 1M1, Canada;* orcid.org/0000-0001-5486-2755; Email: cdrennan@mit.edu

Authors

Steven E. Cohen − *Department of Chemistry, Massachusetts Institute of Technology, Cambridge, Massachusetts 02139, United States;* orcid.org/0000-0002-3193-0740

Mehmet Can − *Department of Biological Chemistry, University of Michigan Medical School, Ann Arbor, Michigan 04109, United States*

Elizabeth C. Wittenborn − *Department of Chemistry, Massachusetts Institute of Technology, Cambridge, Massachusetts 02139, United States;* orcid.org/0000-0002-8473-0814

Rachel A. Hendrickson − *Department of Biology, Massachusetts Institute of Technology, Cambridge, Massachusetts 02139, United States*

Stephen W. Ragsdale − *Department of Biological Chemistry, University of Michigan Medical School, Ann Arbor, Michigan 04109, United States;* orcid.org/0000-0003-3938-8906

Complete contact information is available at: https://pubs.acs.org/10.1021/acscatal.0c03033

Notes

The authors declare no competing financial interest.

Atomic coordinates and structure factors have been deposited in the Protein Data Bank (www.rcsb.org) under the following accession code: 6X5K.

■ ACKNOWLEDGMENTS

We are grateful to Surajit Banerjee for help with EDS data analysis. This work was supported by NIH Grants T32 GM008334 (S.E.C. and E.C.W.), R35 GM126982 (C.L.D.), and R37 GM039451 to (S.W.R.). S.E.C. is a recipient of a Martin Family Society Fellowship for Sustainability. C.L.D. is a Howard Hughes Medical Institute Investigator and a fellow of the Bioinspired Solar Energy Program, Canadian Institute for Advanced Research. This work is based on research conducted at the Advanced Photon Source on the Northeastern Collaborative Access Team beamlines, which are funded by the National Institute of General Medical Sciences from the NIH (P30 GM124165). The Pilatus 6M detector on beamline 24-ID-C is funded by a NIH Office of Research Infrastructure Programs High End Instrumentation grant (S10 RR029205). This research used resources of the Advanced Photon Source, a U.S. Department of Energy (DOE) Office of Science User Facility operated for the DOE Office of Science by Argonne National Laboratory under Contract No. DE-AC02-06CH11357.

■ ABBREVIATIONS

CODH, carbon monoxide dehydrogenase; ACS, acetyl-CoA synthase; CFeSP, corrinoid iron−sulfur protein; EPR, electron paramagnetic resonance; EXAFS, extended X-ray absorption fine structure; EDS, energy dispersion X-ray spectroscopy

■ REFERENCES

(1) Drake, H. L. Acetogenesis, Acetogenic Bacteria, and the Acetyl-CoA "Wood/Ljungdahl" Pathway: Past and Current Perspectives. In *Acetogenesis*; Drake, H. L., Ed.; Chapman & Hall: New York, 1994; pp 3−60.

(2) Diekert, G. B.; Thauer, R. K. Carbon monoxide oxidation by *Clostridium thermoaceticum* and *Clostridium formicoaceticum*. *J. Bacteriol.* **1978**, *136*, 597−606.

(3) Doukov, T. I.; Iverson, T. M.; Seravalli, J.; Ragsdale, S. W.; Drennan, C. L. A Ni-Fe-Cu center in a bifunctional carbon monoxide dehydrogenase/acetyl-CoA synthase. *Science* **2002**, *298*, 567−72.

(4) Doukov, T. I.; Blasiak, L. C.; Seravalli, J.; Ragsdale, S. W.; Drennan, C. L. Xenon in and at the end of the tunnel of bifunctional carbon monoxide dehydrogenase/acetyl-CoA synthase. *Biochemistry* **2008**, *47*, 3474−83.

(5) Hu, S. I.; Drake, H. L.; Wood, H. G. Synthesis of acetyl coenzyme A from carbon monoxide, methyltetrahydrofolate, and coenzyme A by enzymes from *Clostridium thermoaceticum*. *J. Bacteriol.* **1982**, *149*, 440−8.

(6) Hu, S. I.; Pezacka, E.; Wood, H. G. Acetate synthesis from carbon monoxide by *Clostridium thermoaceticum*. Purification of the corrinoid protein. *J. Biol. Chem.* **1984**, *259*, 8892−7.

(7) Pezacka, E.; Wood, H. G. Role of carbon monoxide dehydrogenase in the autotrophic pathway used by acetogenic bacteria. *Proc. Natl. Acad. Sci. U. S. A.* **1984**, *81*, 6261−5.

(8) Appel, A. M.; Bercaw, J. E.; Bocarsly, A. B.; Dobbek, H.; DuBois, D. L.; Dupuis, M.; Ferry, J. G.; Fujita, E.; Hille, R.; Kenis, P. J.; Kerfeld, C. A.; Morris, R. H.; Peden, C. H.; Portis, A. R.; Ragsdale, S. W.; Rauchfuss, T. B.; Reek, J. N.; Seefeldt, L. C.; Thauer, R. K.; Waldrop, G. L. Frontiers, opportunities, and challenges in biochemical and chemical catalysis of CO2 fixation. *Chem. Rev.* **2013**, *113*, 6621−58.

(9) Can, M.; Armstrong, F. A.; Ragsdale, S. W. Structure, function, and mechanism of the nickel metalloenzymes, CO dehydrogenase, and acetyl-CoA synthase. *Chem. Rev.* **2014**, *114*, 4149−74.
(10) Kung, Y.; Drennan, C. L. A role for nickel-iron cofactors in biological carbon monoxide and carbon dioxide utilization. *Curr. Opin. Chem. Biol.* **2011**, *15*, 276−83.
(11) Ragsdale, S. W.; Ljungdahl, L. G.; DerVartanian, D. V. Isolation of carbon monoxide dehydrogenase from *Acetobacterium woodii* and comparison of its properties with those of the *Clostridium thermoaceticum* enzyme. *J. Bacteriol.* **1983**, *155*, 1224−37.
(12) Ragsdale, S. W.; Wood, H. G.; Antholine, W. E. Evidence that an iron-nickel-carbon complex is formed by reaction of CO with the CO dehydrogenase from *Clostridium thermoaceticum*. *Proc. Natl. Acad. Sci. U. S. A.* **1985**, *82*, 6811−4.
(13) Lindahl, P. A.; Ragsdale, S. W.; Munck, E. Mossbauer study of CO dehydrogenase from *Clostridium thermoaceticum*. *J. Biol. Chem.* **1990**, *265*, 3880−8.
(14) Bramlett, M. R.; Tan, X.; Lindahl, P. A. Inactivation of acetyl-CoA synthase/carbon monoxide dehydrogenase by copper. *J. Am. Chem. Soc.* **2003**, *125*, 9316−7.
(15) Gencic, S.; Grahame, D. A. Nickel in subunit beta of the acetyl-CoA decarbonylase/synthase multienzyme complex in methanogens. Catalytic properties and evidence for a binuclear Ni-Ni site. *J. Biol. Chem.* **2003**, *278*, 6101−10.
(16) Seravalli, J.; Xiao, Y.; Gu, W.; Cramer, S. P.; Antholine, W. E.; Krymov, V.; Gerfen, G. J.; Ragsdale, S. W. Evidence that NiNi acetyl-CoA synthase is active and that the CuNi enzyme is not. *Biochemistry* **2004**, *43*, 3944−55.
(17) Darnault, C.; Volbeda, A.; Kim, E. J.; Legrand, P.; Vernede, X.; Lindahl, P. A.; Fontecilla-Camps, J. C. Ni-Zn-[Fe4-S4] and Ni-Ni-[Fe4-S4] clusters in closed and open subunits of acetyl-CoA synthase/carbon monoxide dehydrogenase. *Nat. Struct. Mol. Biol.* **2003**, *10*, 271−9.
(18) Svetlitchnyi, V.; Dobbek, H.; Meyer-Klaucke, W.; Meins, T.; Thiele, B.; Romer, P.; Huber, R.; Meyer, O. A functional Ni-Ni-[4Fe-4S] cluster in the monomeric acetyl-CoA synthase from *Carboxydothermus hydrogenoformans*. *Proc. Natl. Acad. Sci. U. S. A.* **2004**, *101*, 446−51.
(19) Can, M.; Giles, L. J.; Ragsdale, S. W.; Sarangi, R. X-ray Absorption Spectroscopy Reveals an Organometallic Ni-C Bond in the CO-Treated Form of Acetyl-CoA Synthase. *Biochemistry* **2017**, *56*, 1248−1260.
(20) Gencic, S.; Duin, E. C.; Grahame, D. A. Tight coupling of partial reactions in the acetyl-CoA decarbonylase/synthase (ACDS) multienzyme complex from *Methanosarcina thermophila*: acetyl C-C bond fragmentation at the a cluster promoted by protein conformational changes. *J. Biol. Chem.* **2010**, *285*, 15450−63.
(21) Fan, C. L.; Gorst, C. M.; Ragsdale, S. W.; Hoffman, B. M. Characterization of the Ni-Fe-C complex formed by reaction of carbon monoxide with the carbon monoxide dehydrogenase from *Clostridium thermoaceticum* by Q-band ENDOR. *Biochemistry* **1991**, *30*, 431−5.
(22) Kumar, M.; Ragsdale, S. W. Characterization of the Co Binding-Site of Carbon-Monoxide Dehydrogenase from *Clostridium thermoaceticum* by Infrared-Spectroscopy. *J. Am. Chem. Soc.* **1992**, *114*, 8713−8715.
(23) Kung, Y.; Doukov, T. I.; Seravalli, J.; Ragsdale, S. W.; Drennan, C. L. Crystallographic snapshots of cyanide- and water-bound C-clusters from bifunctional carbon monoxide dehydrogenase/acetyl-CoA synthase. *Biochemistry* **2009**, *48*, 7432−40.
(24) Volbeda, A.; Fontecilla-Camps, J. C. Crystallographic evidence for a CO/CO2 tunnel gating mechanism in the bifunctional carbon monoxide dehydrogenase/acetyl coenzyme A synthase from *Moorella thermoacetica*. *JBIC, J. Biol. Inorg. Chem.* **2004**, *9*, 525−532.
(25) Seravalli, J.; Ragsdale, S. W. Pulse-chase studies of the synthesis of acetyl-CoA by carbon monoxide dehydrogenase/acetyl-CoA synthase: evidence for a random mechanism of methyl and carbonyl addition. *J. Biol. Chem.* **2008**, *283*, 8384−94.
(26) Maynard, E. L.; Sewell, C.; Lindahl, P. A. Kinetic mechanism of acetyl-CoA synthase: steady-state synthesis at variable CO/CO2 pressures. *J. Am. Chem. Soc.* **2001**, *123*, 4697−703.
(27) Hegg, E. L. Unraveling the structure and mechanism of acetyl-coenzyme A synthase. *Acc. Chem. Res.* **2004**, *37*, 775−83.
(28) Ragsdale, S. W. Life with carbon monoxide. *Crit. Rev. Biochem. Mol. Biol.* **2004**, *39*, 165−95.
(29) Lindahl, P. A. The Ni-containing carbon monoxide dehydrogenase family: light at the end of the tunnel? *Biochemistry* **2002**, *41*, 2097−105.
(30) Ragsdale, S. W.; Ljungdahl, L. G.; DerVartanian, D. V. EPR evidence for nickel-substrate interaction in carbon monoxide dehydrogenase from *Clostridium thermoaceticum*. *Biochem. Biophys. Res. Commun.* **1982**, *108*, 658−63.
(31) Seravalli, J.; Kumar, M.; Ragsdale, S. W. Rapid kinetic studies of acetyl-CoA synthesis: evidence supporting the catalytic intermediacy of a paramagnetic NiFeC species in the autotrophic Wood-Ljungdahl pathway. *Biochemistry* **2002**, *41*, 1807−19.
(32) George, S. J.; Seravalli, J.; Ragsdale, S. W. EPR and infrared spectroscopic evidence that a kinetically competent paramagnetic intermediate is formed when acetyl-coenzyme A synthase reacts with CO. *J. Am. Chem. Soc.* **2005**, *127*, 13500−1.
(33) Manesis, A. C.; Musselman, B. W.; Keegan, B. C.; Shearer, J.; Lehnert, N.; Shafaat, H. S. A Biochemical Nickel(I) State Supports Nucleophilic Alkyl Addition: A Roadmap for Methyl Reactivity in Acetyl Coenzyme A Synthase. *Inorg. Chem.* **2019**, *58*, 8969−8982.
(34) Manesis, A. C.; O'Connor, M. J.; Schneider, C. R.; Shafaat, H. S. Multielectron Chemistry within a Model Nickel Metalloprotein: Mechanistic Implications for Acetyl-CoA Synthase. *J. Am. Chem. Soc.* **2017**, *139*, 10328−10338.
(35) Manesis, A. C.; Shafaat, H. S. Electrochemical, Spectroscopic, and Density Functional Theory Characterization of Redox Activity in Nickel-Substituted Azurin: A Model for Acetyl-CoA Synthase. *Inorg. Chem.* **2015**, *54*, 7959−67.

https://dx.doi.org/10.1021/acscatal.0c03033
ACS Catal. 2020, 10, 9741−9746